

X-ray diffraction analysis of the defect structure in $\text{Al}_x\text{Ga}_{1-x}\text{N}$ films grown by metalorganic chemical vapor deposition

Y. S. PARK*, K. H. KIM, J. J. LEE, H. S. KIM

Department of Physics and Research Institute of Natural Science, Gyeongsang National University, Jinju 660-701, Korea

E-mail: yspark@dongguk.edu

E-mail: hskim@nongae.gsnu.ac.kr

T. W. KANG

Quantum Functional Semiconductor Research Center, Dongguk University, Seoul 100-715, Korea

H. X. JIANG, J. Y. LIN

Department of Physics, Kansas State University, Manhattan, KS 66506, USA

Most of the GaN and related alloy materials used for device development are epitaxially grown on sapphire. Because of the large lattice mismatch (14%) between GaN and sapphire, a thin, highly dislocated region is generated at the layer/substrate interface to relieve the strain, and the structural properties of this interface region have been studied in great detail [1]. Moreover, the difference of thermal expansion coefficients and lattice constants between GaN and Al_2O_3 , induce crystal defects such as micro-cracks, micro-pipes and mosaic structures which affect the physical properties of the GaN films [2]. Commonly, axis reflections of high intensity are measured (i.e., (001) reflections for (001)-oriented epilayer, for example) and their full width at half maximum (FWHM) values are taken as a figure of merit for the crystalline perfection which is supported by theoretical models [3]. In contrast to that, the estimation of total dislocation densities in (001) oriented GaN epitaxial layers requires measuring (hkl) reflections with h or $k \neq 0$ [4]. Such measurements were recently reported for series of GaN layers grown by hydride vapor phase epitaxy (HVPE) [5] and metal organic chemical vapor deposition (MOCVD) [6]. However, systematic studies of the relationship between (001) and (hkl) X-ray diffraction (XRD) profiles have not been reported. In this study, we report the reduction of the defects in $\text{Al}_x\text{Ga}_{1-x}\text{N}$ films by increasing Al content.

The $\text{Al}_x\text{Ga}_{1-x}\text{N}$ films of 1 μm thickness were grown by MOCVD on sapphire (0001) substrates with 20 nm low temperature GaN buffer layers. Trimethylgallium (TMGa) and trimethylaluminum (TMAI) were used as metal organic sources. The nitrogen source used was ammonia (NH_3). The Al content (x) of $\text{Al}_x\text{Ga}_{1-x}\text{N}$ films was controlled by the TMAI and TMGa flow rates, and was determined from X-ray diffraction (XRD) spectra by using Vegard's law [7]. Also the grain size of $\text{Al}_x\text{Ga}_{1-x}\text{N}$ films was calculated by using XRD technique.

According to the XRD theory [8, 9] with mosaic structure, the FWHM were determined by distribution

of crystal direction, distribution of the lattice spacing, and superposition of finite crystal size. The grain size of the crystal, L , can be estimated by the relation given by Scherrer [10, 11].

$$L = \frac{K\lambda}{\Delta\theta_{2\theta} \cos \theta} \quad (1)$$

where λ is the wavelength of the incident X-rays and K is 0.7 [11–13] for micro-crystallinity and 0.89 [14] for thin film, respectively. $\Delta\theta_{2\theta}$ is FWHM of Bragg's angle, and can be calculated by the following equation:

$$\Delta\theta_{2\theta}^2 = \Delta\theta_M^2 - \Delta\theta_s^2 \quad (2)$$

where $\Delta\theta_M$ and $\Delta\theta_s$ is the FWHM of sample and standard sample, respectively. We used the Al_2O_3 (0001) as standard sample for growing the $\text{Al}_x\text{Ga}_{1-x}\text{N}$.

Fig. 1a shows the $\theta/2\theta$ -scan XRD spectrum of Al_2O_3 substrate. We can observe the two peaks according to $\text{Cu K}\alpha_1$ and $\text{Cu K}\alpha_2$ of X-ray source and well resolved by pseudo-Voigt function fitting. In Fig. 1a closed square is the measured data, dash and dot line are new reconstructed peaks. The FWHM of Al_2O_3 is 0.04° due to $\text{Cu K}\alpha_1$. From the same fitting method, $\text{Al}_x\text{Ga}_{1-x}\text{N}$ samples were fitted and the FWHM were calculated 0.11° for GaN (In Fig. 1b) and 0.08° for $\text{Al}_{0.13}\text{Ga}_{0.87}\text{N}$ (In Fig. 1c).

Fig. 2 shows the θ -rocking curve of $\text{Al}_x\text{Ga}_{1-x}\text{N}$ films for (0002) plane. The FWHM and grain size are summarized in Table I. The FWHM of θ -rocking curve increases with Al content, but the grain size increases with Al content. Despite the large FWHM of the θ -rocking curve for samples with high Al contents, the grain size is larger than the GaN. This means that the crystal quality of c -plane decreases with increasing Al content. The grain is related to defects such as threading dislocations. As usual, the GaN epitaxial films have a specific defect structure consisting of dislocation ensembles and so-called columns. An etched grain is

* Present address: QSRC in Dongguk University.

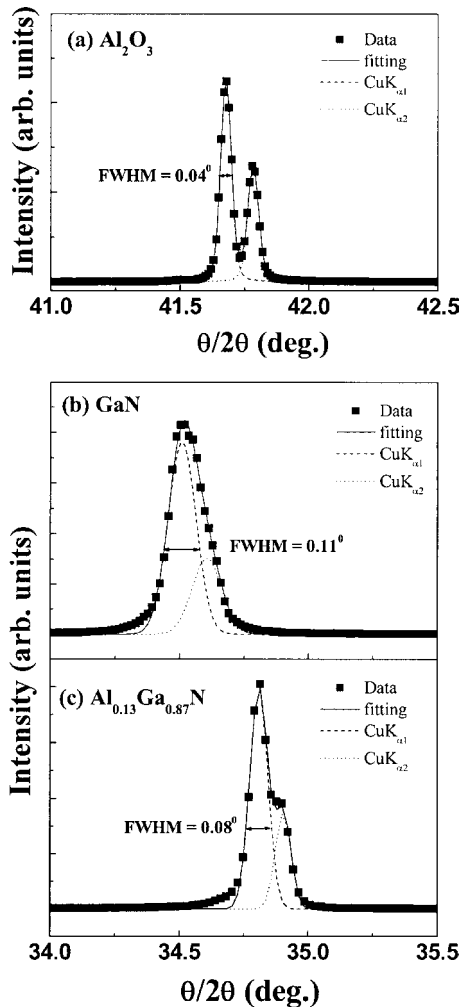


Figure 1 X-ray diffraction profiles in the $\theta/2\theta$ mode of $\text{Al}_x\text{Ga}_{1-x}\text{N}$ films: (a) Al_2O_3 , (b) GaN and (c) $\text{Al}_{0.13}\text{Ga}_{0.87}\text{N}$. The closed squares are the data, dashed line is $\text{CuK}_{\alpha 1}$, dot line is $\text{CuK}_{\alpha 2}$, and solid line is simulated result from $\text{CuK}_{\alpha 1}$ and $\text{CuK}_{\alpha 2}$.

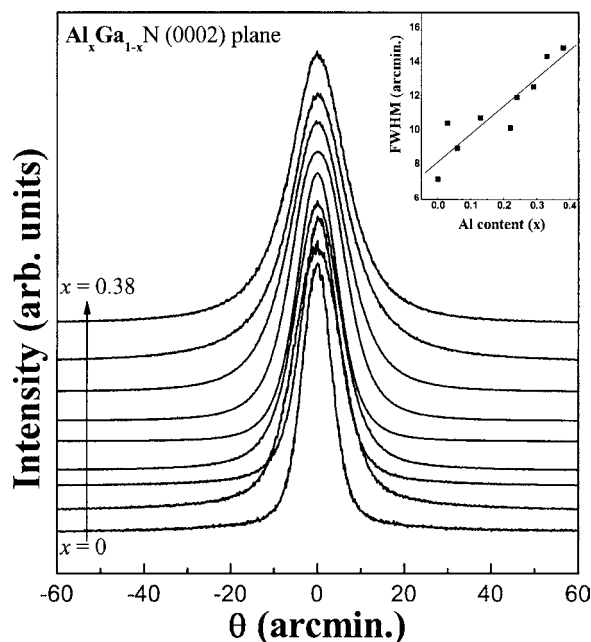


Figure 2 The X-ray θ -rocking curve of $\text{Al}_x\text{Ga}_{1-x}\text{N}$ films. The inserts show the FWHM of θ -rocking curve.

TABLE I The FWHM of θ -rocking curve and grain size from calculated by Scherrer equation

Sample (x)	θ (arcmin.)	$\theta/2\theta$ (deg.)	Grain size (\AA)
0.00	6.8	0.110	884
0.03	8.5	0.098	1013
0.06	9.1	0.094	1065
0.13	10.8	0.080	1308
0.20	10.2	0.066	1727
0.24	12.0	0.101	980
0.29	12.6	0.098	1020
0.33	14.4	0.103	960
0.38	14.9	0.102	965

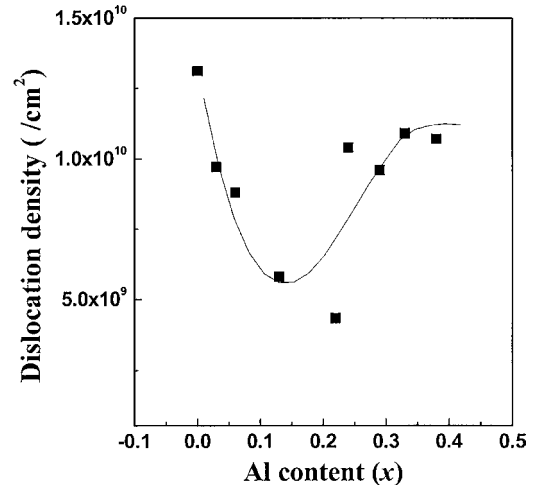


Figure 3 The dislocation density of $\text{Al}_x\text{Ga}_{1-x}\text{N}$ films as a function of Al content.

associated with a dislocation which twists (tilts) the grain with respect to its neighbors. It has been noted that grain boundaries between grains, as in mosaic structural material, arise only if arrays of dislocations are formed. The grain size was calculated and the values ranged about 850–2000 \AA , with increasing Al contents. This values are in good agreement with those reported by Koide [9] and Wang [15].

Fig. 3 shows the dislocation density as a function of Al contents. As shown in Fig. 3, the dislocation densities decrease with increasing Al content up to 0.2. Thus it is concluded that a large grain size (or decreased dislocation density) can be obtained via increase of Al content. This is described by a linear relationship between peak width and dislocation density. Bottcher *et al.* [16] have reported that the edge dislocation density is significantly influenced by the average grain diameter, being approximately proportional to the inverse grain diameter. The dislocation density was deduced as a function of Al content from the linear relation of the grain size and the values fall in the range of 10^9 – $10^{10}/\text{cm}^2$. The dislocation density decreases with increasing Al contents up to 0.2. In order to reduce the threading dislocation density, Kashima *et al.* [17] have used an AlN interlayer during the GaN growth. The Ga vacancies could be totally replaced by the diffused Al, even through only one sixth of the Al can substitute for the same group-III Ga atoms. It is noted that for the epitaxy methods, such as MOCVD and HVPE, rather high

temperatures (higher than 800°C) are required for growth. At such sustained elevated temperatures ($T = 1060^\circ\text{C}$ for MOCVD), atomic diffusion would appear to be a dominant process associated with the film's growth allowing Al atoms to diffuse and fill the Ga sites in the near-interface region in the film. Also, Xu *et al.* [18] have reported that most Ga vacancy sites are replaced by the group-III element Al at the interface. This follows not only from the copious amount of Al present at the interface, but also from the fact that Al has similar chemistry to Ga.

Acknowledgments

This work was supported by the Korea Research Foundation under Grant No. KRF-2000-042-D00026 and by the Korea Science and Engineering Foundation through the QSRC in Dongguk University.

References

1. D. C. LOOK and R. J. MOLNAR, *Appl. Phys. Lett.* **70** (1997) 3377.
2. B. N. SVERDLOV, G. A. MARTIN, D. T. SMITH and H. MORKOC, *ibid.* **67** (1995) 2063.
3. V. M. KAGANER, R. KOHLER, M. SCHMIDBAUER, R. OPITZ and B. JENICHEN, *Phys. Rev. B* **55** (1997) 1793.
4. Q. ZHU, A. BOTCHKAREV, W. KIM, O. AKTAS, A. SALVADOR, B. SVERDLOV, H. MORKOC, S.-C. Y. TSEN and D. J. SMITH, *Appl. Phys. Lett.* **68** (1996) 1141.
5. Y. GOLAN, X. H. WU, J. S. SPECK, R. P. VAUDO and V. M. PHANSE, *ibid.* **73** (1998) 3090.
6. K. S. KIM, C. S. OH, K. J. LEE, G. M. YANG, C.-H. HONG, K. Y. LIM, H. J. LEE and A. YOSHIKAWA, *J. Appl. Phys.* **85** (1999) 8441.
7. L. VEGARD, *Z. Phys.* **5** (1921) 17.
8. N. ITOH and K. OKAMOTO, *J. Appl. Phys.* **63** (1988) 1486.
9. Y. KOIDE, K. ITOH, N. SAWAKI and I. AKASAKI, *Jpn. J. Appl. Phys.* **27** (1988) 1156.
10. P. SCHERRER, *Göttinger Nachr.* **2** (1918) 98.
11. A. OHTANI, K. S. STEVENS and R. BERESFORD, *Appl. Phys. Lett.* **65** (1994) 61.
12. A. L. PATTERSON, *Z. Kristallogr.* **66** (1928) 637.
13. F. W. JONES, *Proc. Roy. Soc. London, Ser. A* **166** (1938) 16.
14. W. L. BRAGG, "The Crystalline States" (A. General Survey, Vol. I, Bell, London, 1919) p. 189.
15. L. WANG, X. LIU, Y. ZAN, D. WANG, D. C. LU, Z. WANG, Y. WANG, L. CHENG and Z. ZHANG, *J. Cryst. Growth* **193** (1998) 484.
16. T. BOTTCHER, S. EINFELDT, S. FIGGE, R. CHERCHIA, H. HEINKE, D. HOMMEL and J. S. SPECK, *Appl. Phys. Lett.* **78** (2001) 1976.
17. T. KASHIMA, R. NAKAMURA, M. IWAYA, H. KATOH, S. YAMAGUCHI, H. A. AMANO and I. AKASAKI, *Jpn. J. Appl. Phys.* **38** (1999) L1515.
18. X. L. XU, C. D. BELING, S. FUNG, Y. W. ZHAO, N. F. SUN, T. N. SUN, Q. L. ZHANG, H. H. ZHAN, B. Q. SUN, J. N. WANG, W. K. GE and P. C. WONG, *Appl. Phys. Lett.* **76** (2000) 151.

*Received 11 August
and accepted 26 September 2003*